

# Catalysis Science & Technology

Accepted Manuscript



This is an *Accepted Manuscript*, which has been through the Royal Society of Chemistry peer review process and has been accepted for publication.

*Accepted Manuscripts* are published online shortly after acceptance, before technical editing, formatting and proof reading. Using this free service, authors can make their results available to the community, in citable form, before we publish the edited article. We will replace this *Accepted Manuscript* with the edited and formatted *Advance Article* as soon as it is available.

You can find more information about *Accepted Manuscripts* in the [Information for Authors](#).

Please note that technical editing may introduce minor changes to the text and/or graphics, which may alter content. The journal's standard [Terms & Conditions](#) and the [Ethical guidelines](#) still apply. In no event shall the Royal Society of Chemistry be held responsible for any errors or omissions in this *Accepted Manuscript* or any consequences arising from the use of any information it contains.

## MINIREVIEW

## Emerging Strategies of Breaking 3D Amorphous Network of Lignin

Cite this: DOI: 10.1039/x0xx00000x

Saikat Dutta,\*<sup>a</sup> Kevin C.-W. Wu,\*<sup>a</sup> Basudeb Saha\*<sup>bc</sup>Received 00th January 2012,  
Accepted 00th January 2012

DOI: 10.1039/x0xx00000x

www.rsc.org/

Representing a complex polymeric and amorphous structure arising from enzymatic dehydrogenative polymerization of three phenylpropanoid monomers, namely, synapyl alcohol, coniferyl alcohol, and *p*-cumaryl alcohol, lignin is mainly spotted as an integral part of the secondary cell walls of lignocellulosic biomass such as plant and algae. The absence of commercial high-value application of lignin is mainly due to its heterogeneous molecular structure which has built formidable challenges for developing depolymerization techniques and adequate structural modifications. Lignin valorization represents an important challenge in biorefinery. In this perspective, emerging trends in lignin valorization to derive chemicals and materials are presented with a major focus on critical aspects of dehydrogenation/hydrogenolysis, deoxygenation, enzymatic oxidation, and carbonization. In most cases, conversion of suitable lignin model compounds and actual lignin samples are emphasized. Major focus is given for evaluating the nanoscale structure of employed catalysts for dehydrogenation and deoxygenation techniques. Scope of accessing hierarchically porous carbon materials of fiber and particle morphology via carbonization of lignin is also emphasized. By analyzing the current situation in lignin valorization, certain realistic future directions are sorted and emphasized.

## 1. Introduction

Human beings are desperate to replace source of energy and materials, i. e. petroleum oil with biomass which has been solely used so far by other living organisms for the production of high-energy compounds such as ATP and a wide range of polymers such as DNA, proteins and polysaccharides for millions of years. In the context of being a key component in plant cell wall and most abundant renewable aromatic polymer, lignin has yet to play a significant role as feedstock. Lignin composes ~25% of lignocellulosic biomass and it is an amorphous natural polymer consisting of 3D arrangement of methoxylated phenylpropane.<sup>1</sup> The complex structure of lignin is amorphous, polyaromatic and incorporated with numerous ether linkages, -OH, and methoxy groups. Lignin is regarded as cross-linked macromolecule composed of three types of monolignol, including *p*-coumaryl alcohol, coniferyl alcohol, and synapyl alcohol with the proportions depending on the source.<sup>2</sup> For example, lignin from softwood consists largely of coniferyl units (4-(3-hydroxy-1-proenyl)-2-methoxyphenol) whereas hardwoods consist largely of syringol (2,6-dimethoxyphenol) units excluding exceptions. The *p*-coumaryl units without methoxy groups on the aromatic ring, are also found in lignin. Moreover, coniferyl, syringol, and *p*-cumaryl units are interconnected through various cross-linkages (C-O-C =  $\beta$ -O-4,  $\alpha$ -O-4, 4-O-5) and C-C interunit linkages ( $\beta$ -1  $\beta$ -5,  $\beta$ - $\beta$ , 5-5) as formed during the biosynthesis of macromolecular

lignin (Figure 1) of which the most abundant being the  $\beta$ -O-4 ether linkage.<sup>3</sup> It is essential to understand the details of linkages present in the macromolecular structure in order to design strategies for selective breaking of these linkages. The essential difference between lignin in hardwoods and softwoods is the number of methoxy groups on the aryl rings. Hardwood contains two or three methoxy groups per aromatic rings originated from coniferyl and syringol alcohol units however softwoods contains only one methoxy groups originates from the polymerization of coniferyl alcohol.<sup>4</sup> The common linkage between the monomers is the  $\beta$ -O-4, represents approximately 50-65% of all inter subunit bonds (Table 1).

**Table 1.** Types and frequencies (%) of inter-subunit linkages in softwood and hardwood lignin.<sup>5</sup>

	Linkage	Softwood Lignin	Hardwood Lignin
	$\beta$ -O-4	49-51	65
	$\alpha$ -O-4	6-8	-
	$\beta$ -5	9-15	6
	$\beta$ -1	2	15
	5-5	9.5	2.3
	4-O-5	3.5	1.5
	$\beta$ - $\beta$	2	5.5

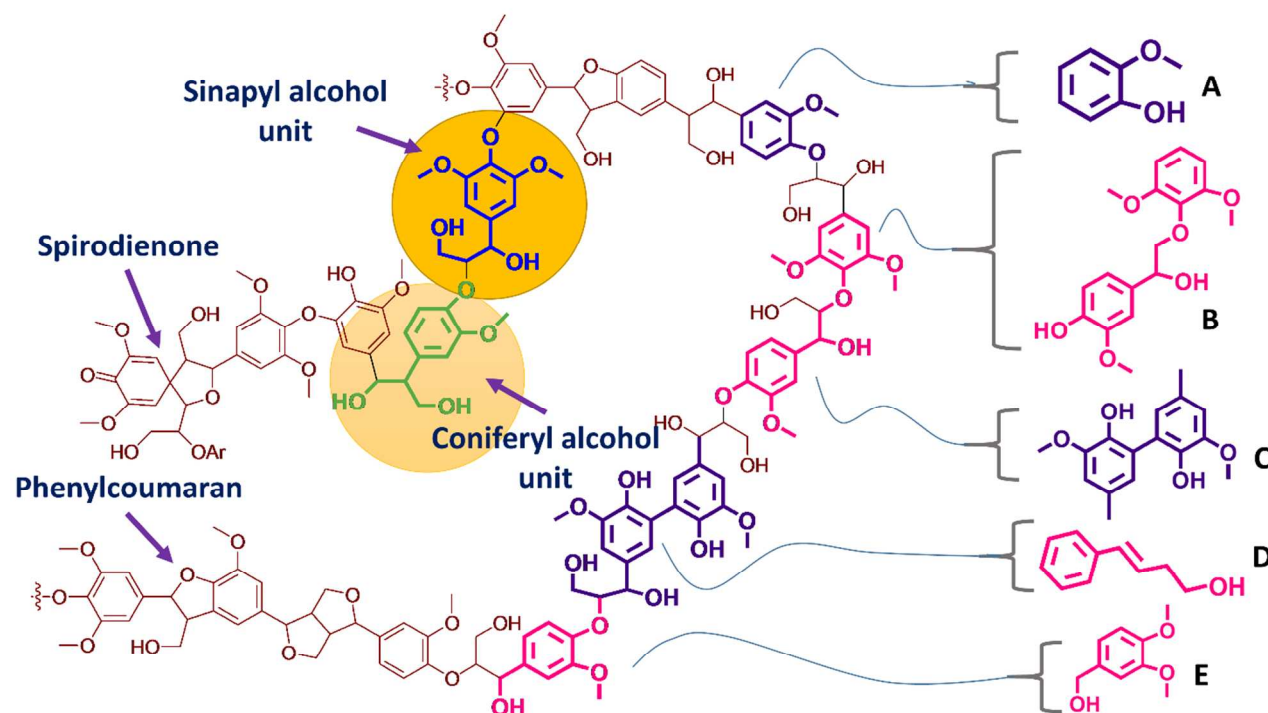


**Figure 1.** Schematic depiction of lignin, showing various linkages and lignin model compounds to model (A) phenol and methoxy functionality, (B)  $\beta$ -O-4 linkages, (C) 5-5' linkages, (D) propyl side chain, and (E) benzylic groups.

The most abundant linkages are  $\beta$ -O-4 and 5-5' constituting approximately 50-65% and 20-25% of structure respectively.<sup>5</sup> Chemical conversion of cellulose and hemicellulose has been extensively studied, while that of lignin remains scarce albeit lignin is the most abundant renewable aromatic polymer, constituting up to 15-30% of the weight and 40% of the energy content of lignocellulosic biomass.<sup>6,7</sup> As we know that due to its rigid cross-linked structure that renders lignin resistant to chemical degradation.

The catalytic valorization of lignin represents a potentially useful method to access bulk and fine chemicals and there are different approaches via chemical routes for developing such processes.<sup>6</sup> Significantly, disruption of linkages of lignin represents a potential route for the production of a wide range of aromatic compounds, which are otherwise accessible only from petroleum feedstocks. The utilization of lignin as feedstock for conversions to hydrocarbons also offers a significant opportunity for enhancing the overall operational efficiency, carbon conversion rate, economic viability, and sustainability of biofuel production.<sup>8</sup> The challenge, however, is the propensity of the aromatic lignin macromolecular assembly to condense and degrade, thereby generating high amounts of relatively intractable solid residues in biorefinery, and paper and pulp industries. Therefore, depolymerization of lignin and its subsequent conversion to value added products is vital to enhance the profitability of biorefineries.<sup>9</sup> Among three main biopolymers that make up the cell wall, lignin is the most recalcitrant. It comprises up to 3% of the plant's mass and is needed for support and water transport.<sup>10</sup> Furthermore, lignin's high aromatic content is responsible for its high energy content. A number of different linkages occur naturally in lignin's structure with the most abundant being the  $\beta$ -O-4 ether linkage (Figure 1).<sup>2</sup> Therefore, methods to break apart lignin 3D network while preserving its aromatic nature promises to provide a valuable stream of chemicals. Previous methods to depolymerize lignin include hydrolysis,<sup>11-13</sup>

pyrolysis,<sup>14,15</sup> catalytic hydrogenation,<sup>16,17</sup> oxidation,<sup>5</sup> hydrocracking.<sup>18</sup> Schinski et al. disclose a process for the hydrotreatment of lignin to yield aromatic products, requiring the use of a hydrogen feedstock.<sup>8,19</sup> Lignin treatment and gasification using supercritical water ( $T_c = 647.3$  K,  $P_c = 221$  bar) have also been reported to primarily form light alkanes and hydrogen,<sup>20-22</sup> although the disadvantages of these processes include the high reaction temperatures and pressures (often T 673 K and P 250 bar).

Lignin is ever underutilized and bulk of produced lignin, representing about 70 million metric tons per year, being only employed as combustible material for its high heat value.<sup>8</sup> Precise control over the techniques to selectively depolymerize lignin is expected to propel the growth of this field further into new realms of synthetic chemistry focused on utilizing lignin as feedstocks. Despite, templating biomaterial is an active area for harnessing the structural complexity to mimic natural functions,<sup>23</sup> disruption of lignin polymeric structure has been of remarkable interest due to following reasons, 1) large reservoir of aromatic hydrocarbons, 2) deoxygenation of ethereal oxygen to obtain hydrocarbons, 3) nanostructured carbon materials or hybrid materials with carbon by strategic carbonization of lignin in/or absence of structure/pore directing templates. Considering above facts, this perspective focuses on describing structural features of recalcitrant lignin in the woody biomass. To further, we picked the essence of emerging strategies of lignin valorization and mainly its chemical aspects for example, hydrodeoxygenation, synthetic biological methods, and carbonization for novel porous carbon materials. Major emphasis is invested on the chemicals and material aspects of these techniques which promise to create significant impact in lignin valorization. Lignin model reaction to understand the underlying features of depolymerization and selective cleavage of a bond present is described with important recently reported cases in all sections of emerging lignin valorization. Future prospects of lignin valorization and possible new techniques are also proposed.

## 2. Emerging Lignin Valorization Techniques

Considering lignin as renewable reservoir of aromatic building blocks, breaking of complex crosslinked polymeric units via selective inter-unit C–O–C bond cleavage and subsequent hydrodeoxygenation of the low molecular weight moieties to aromatic and aliphatic hydrocarbons is an emerging strategy. It is to create avenues through the chemical and biological conversion of lignin to chemicals and fuels. Despite the potential, the conversion of lignin to liquid fuels, particularly to aliphatic and aromatic hydrocarbons has always been a challenging task. Generally, propensity of the aromatic lignin macromolecular assembly condense and degrade via generating high amounts of relatively intractable solid residues in biorefinery processes. Among the recently developed processes, hydrogenolysis of C–O bonds results breakdown of high molecular weight components and this process offers phenols as end product. However, in order to access liquid hydrocarbon, recently hydrodeoxygenation technique under hydrogenolytic condition has gained tremendous importance. This techniques required noble metal nanoparticle catalyst and in most of the cases, biofunctional or bimetallic metal nanoparticles exhibited remarkable performance as compared to their mononuclear counter part. Liquid phase oxidation of lignin which is mainly dependent on benzylic C–H or C–OH bond transformation to carbonyl groups which process depends on metal catalysts,<sup>6,24</sup> however metal free catalysts are also known now.<sup>25</sup> Enzymatic hydrolysis being a promising strategy for the cellulose degradation, similarly enzymatic oxidation can be considered as a major future prospect for lignin valorization and for the production of aromatics. The essential would be to discover lignin sources which has potential to provide ordered porous carbons directly and among which accessing 3D interconnected porous carbon is one of the major targets. This area of considering lignin as a major source materials used for advanced applications and this also offers ample scope to develop non-templating strategy of deriving materials from renewable source.

### 2.1 Lignin Depolymerization into Monomers

Lignin depolymerization (LDP) into aromatic products under mild conditions is a desired approach for its valorization. So far hydrolysis, oxidation, and reduction are well-established methods, in which, aqueous phase alkali hydroxide or carbonate catalysed hydrolysis of C–O–C linkages results phenol derivatives.<sup>26–28</sup> Oxidative cleavage of C–H bonds and/or C–C bonds adjacent to C–O–C linkages produces vanillin and its analogues.<sup>29,30</sup> This reaction causes oxidative damage to the aromatic fragments of the lignin, leading to extreme oxidation to CO<sub>x</sub> and H<sub>2</sub>O. Beside, vaniline would repolymerize into oligomers leading to poor recovery of depolymerisation products. Reductive depolymerization has been considered as a promising method of LDP to phenols. With hydrogenation or hydrogenolysis methods, C–O–C linkages are selectively cleaved into phenols.<sup>31</sup> The reduction method may partially avoid the condensation of phenol intermediates to oligomers, a key issue associated with the LDP reaction.<sup>32</sup> Kou et al. have reported that lignin is hydrogenated to monomeric phenols over noble metal catalysts mainly consist of Pt, Ru, Pd, and Rh supported on activated carbon under 4 MPa H<sub>2</sub>.<sup>33</sup> Zhang et al. have shown that woody lignin is catalytically hydrogenated to phenolic compounds like guaiacol and syringols.<sup>34</sup> Alternatives such as CuCr oxide,<sup>35</sup> Co–Mo–S/Al<sub>2</sub>O<sub>3</sub>,<sup>36</sup> activated carbon-, alumina- or silica-supported Ru<sup>37</sup> or Pt<sup>38</sup> have also been examined to obtain monomeric phenols via hydrogenation of lignin or model compounds. A strategy of conversion of

lignosulfonate into 4-ethylguaiacol and 4-propylguaiacol over heterogeneous nickel catalysts revealed that aryl–O–alkyl bonds (C–O–C) and hydroxyl groups of lignin are hydrogenated to phenols and alkanes, respectively, while preserving the aromatic structure.<sup>39</sup> When insoluble solid lignin meets heterogeneous catalysts in common solvents, mass transfer becomes limited and may retard the process. Generally, in case of heterogeneously catalyzed conversion of native lignin failed to address the key chemical aspects of the process and thus the problem is far less elucidated. Fragmentation–hydrogenolysis are the key steps occurs in depolymerizing native lignin into monomeric phenols in alcoholic solvents over nickel-based catalysts (Figure 2).<sup>40</sup> The best selectivity toward monomeric phenol products is > 90% from about 50% conversion of birch wood lignin. It is demonstrated that nickel-based catalysts are highly active and selective in native lignin conversion into monomeric phenols such as propylguaiacol and propylsyringol. It is shown that alcohols act as the nucleophilic reagent for C–O–C cleavage in alcoholysis and function as the source of active hydrogen in the medium. Results of this study confirmed that conversion of smaller lignin fragments into monomeric phenols under goes β-elimination dehydration coupled with the hydrogenation and subsequent hydrogenolysis.

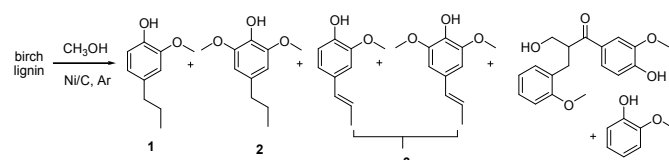


**Figure 2.** β–O–4 Major products in the lignin-depolymerization reaction over the Ni/C catalyst.

In the above discussed depolymerization process efficiency depends on the CH<sub>3</sub>OH as solvent when it comes in contact with active site of catalyst to generate active hydrogen species which energetically favorable than the activation of molecular H<sub>2</sub>. Maximum 54% lignin conversion in methanol can be achieved (Table 2, entry 3) with a total selectivity 89% for the components containing 4-propylguaiacol (PGol) and 4-propylsyringol (PSol) as major products. The Ni/C system for lignin depolymerization also exhibit reusability of at least four times with about ~50% lignin conversion in each cycle. Since Ni forms MeOMe from MeOH and reforms it to H<sub>2</sub>, therefore, CO and CO<sub>2</sub> must be generated in this process as byproducts. The Ni catalyst can also be deactivated in the presence of water. Lignin depolymerization from intact biomass currently produces a largely heterogeneous slate of molecules, which makes lignin valorization an enormously difficult problem. Even after extensive research effort on lignin conversion over the past seven decades, a selective catalyst that narrows the product slate of lignin depolymerization products down to something manageable is yet to be found. The exception is Song's Ni/C-based work, but deactivation of the Ni/C in the presence of water and limitation of strategy with a specific variety of saw dust birch wood are certain downsides of this process.

Non-oxidative degradation involving cleavage of β–O–aryloxy bonds in lignin models has been a standard system to simplify the development for depolymerization of lignin. Recently, vanadium catalyzed β–O–aryloxy bond cleavage in lignin model has been reported which involves formation of enones as a results of C–O bond cleavage

(Scheme 3).<sup>41</sup> Result of this report, reveals the pretreatment and isolation can alter the structure of lignin.

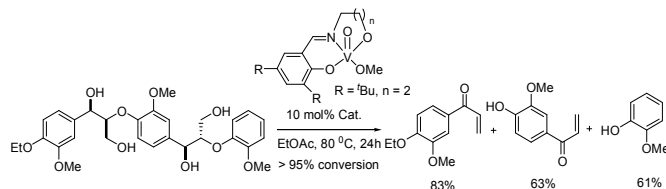


Figure 3.  $\beta$ -O-4 Vanadium-catalyzed degradation of a trimeric lignin model.

Table 2. Catalytic results of the lignin depolymerisation reaction.

Entry	Catalyst	Solvent	Conv. (%)	Selectivity (%)			
				1	2	3	oth ers
1	No cat.	CH <sub>3</sub> OH	n.d.	-	-	-	-
2	AC	CH <sub>3</sub> OH	n.d.	-	-	-	-
3	Ni/C	CH <sub>3</sub> OH	54	22	67	1	10
4	Ni/C	EtOH	48	25	70	3	2
5	Ni/C	EG	50	25	72	1	2
6	Ni/C	i-PrOH	27	12	37	26	25
7	Ni/C	25% glycerol+ H <sub>2</sub> O	16	16	67	-	17
8	Ni/C	1,4- Dioxane	15	-	6	93	<1
9	Ni/C	1% MOH+ H <sub>2</sub> O	9	31	63	-	6
10	Ni/C	25% MeOH+ H <sub>2</sub> O	22	16	74	-	11
11	Ni/C	Cyclohex ane	<1	-	-	-	-
12	Ni/C	MeOH	42	26	71	-	3
13	Ni/SBA- 15	MeOH	27	9	18	72	<1
14	Ni/Al <sub>2</sub> O <sub>3</sub>	MeOH	19	-	18	81	1
15	Cu/C	MeOH	9	-	-	99	1
16	Cu-Cr oxide	MeOH	2	-	-	99	1

Reaction conditions: birch sawdust (2.0 g), catalyst (0.1 g), solvent (40 mL), 200 °C, 6h, 1 atm Ar. n.d.= not detected

1. Propylguaiacol, 2. Propylsyringol, 3. Propenylguaiacol

Production of phenols from lignin via depolymerization techniques clubbed with further conversion (hydrogenolysis or cracking) is a challenging task which has been solved via catalytic cracking and hydrogenolysis involving breakdown of molecular components into small fragments via breaking of C–O bonds in water-alcohol medium which has been suggested as the major reaction route. For these processes of phenol production, tungsten phosphide<sup>42</sup> ZrO<sub>2</sub>-Al<sub>2</sub>O<sub>3</sub>-FeO<sub>x</sub><sup>43</sup> and iron oxide<sup>44</sup> play major role respectively. Depolymerization by catalytic alcoholysis of lignin can offer high-value small molecules of carbons C<sub>6</sub>-C<sub>10</sub> liquid products by using a nanostructured molybdenum carbide catalyst in super

critical ethanol, in which case, advantage is that the lignin fragments can be rapidly stabilized on the surface of catalyst under supercritical condition of ethanol.<sup>45</sup> This recent finding suggest that catalytic alcoholysis is an alternative route to produce value-added chemicals from lignin due to the fact that release of an active hydrogen atom from an alcohol e.g. methanol is more facile than that from a hydrogen molecule. This approach can be regarded as one of the key strategy to derive organic molecules from lignin degradation.

## 2.2 Upgradation of Lignin Monomers

Currently, hydrodeoxygenation (HDO) is receiving more attention which involves complete removal of oxygen atoms from the substrate under hydrogenolytic conditions.<sup>46</sup> Deoxygenation of polyols (e. g. glycerol) to useful organics such as allyl alcohol, propanal, and acrolein is well-established method,<sup>47,48</sup> several catalytic upgrading routes that involve HDO have been widely studied using monomeric lignin model compounds to produce hydrocarbons.<sup>35</sup> HDO has been considered as the major tool to upgrade lignin-derived bio-oils and the HDO process which involves reaction with hydrogen that produce hydrocarbons and water.<sup>49</sup> In order to highlight the importance of HDO reactions in bio-oil upgrading, HDO chemistry of lignin-derived compounds or raw lignin with comparison of activity of employed catalysts is essential. Solid surface that stabilizes water-oil emulsions and catalyze reactions at the liquid/liquid interface, that can lead to biphasic HDO using a deposited Pd onto carbon nanotube-inorganic oxide hybrid, useful for biomass refining as revealed when employed for lignin conversion.<sup>50</sup> The hybrid solid nanoparticle in capable of simultaneously stabilize an emulsion and catalyze reactions in both aqueous and organic phase. In order to removal of oxygenate functional groups in phenolic compounds derived from lignin such as vanillin, the HDO of vanillin by nanohybrid emulsions on Pd was studied as a model reaction performed in aqueous side of the interface where the Pd is deposited in hydrophilic side. As illustrated schematically in Figure 4, a range of different products and phase migration processes occur due to the varying extents of hydrogenation, hydrogenolysis, and decarbonylation of vanillin catalyzed by Pd as the reaction conditions were modified.

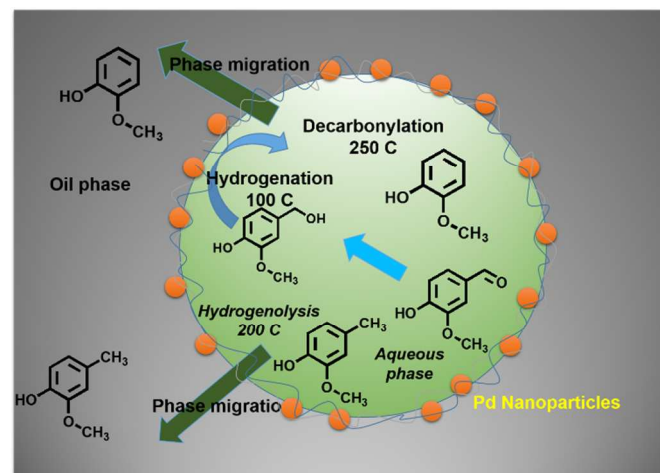


Figure 4. Schematic illustration of the reactions taking place at the water/oil interface in the solid-stabilized emulsions using vanillin as lignin model. Depending on the reaction temperature, the prevailing reactions are hydrogenation, hydrogenolysis, or decarbonylation, and depending on the relative solubility, the products remain in the aqueous phase or migrate to the oil phase.

The major advantage of this method is the solid-stabilized emulsions, a continuous process could be designed in which two homogeneous phases coexist with the emulsion in a layered configuration: oil/emulsion/water. Full conversion can be expected on both sides of the emulsion with constant removal of oil soluble products from the top layer and water soluble products from the bottom layer while reaction is continuous in the emulsion.

In recent years various supported noble metals, such as Ru, Pd, Pt, Rh, and their alloys, have been widely used in aqueous phase non-sulfide-based HDO process for conversion of lignin based monomeric model phenolic substrates to hydrocarbons.<sup>51-53</sup> In the process of hydrotreatment of pyrolysis oil fractions has been considered as promising energy career however chemical aspects of the HDO reactions in fast pyrolysis oil was not investigated in detail even though it was found that the carbohydrate fraction has been very reactive in HDO of pyrolysis oil. It is important to disclose the chemical aspects of the disassembly/“unzipping” process of lignin involving HDO which offers production of value-added products. Recent investigations on model lignin compounds have demonstrated the utility of ruthenium hydrogenation catalysts and nickel carbene hydrogenation catalysts for the hydrogenolysis of the aromatic CO bonds in aryl ethers important for the generation of fuels and chemical feedstocks from lignin. Study on the lignin model compounds revealed the relative reactivity of ether substrates scale as Ar–O–Ar > Ar–OMe > ArCH<sub>2</sub>–OMe (Ar, Aryl; Me, Methyl).<sup>54</sup> Refractory aryl ether biopolymer to hydrocarbon conversion is a formidable challenge to the synthetic chemists. Results from this work have demonstrated that the selective cleavage of aromatic C–O bonds in the presence of other C–O bonds can be conducted without reduction of the arene units although the mechanistic issues are not yet resolved for this nickel system.

Performing HDO to remove covalently bonded oxygen from lignin offers opportunities to not only break apart the lignin's complex structure but also to increase the overall energy density and value of the resulting products. The major complexity is that C–O and C–C bond strengths are comparable, turning selective HDO versus aromatic hydrogenation challenging. There are efforts recently taken for overcoming such critical issues. For example, a bifunctional catalyst constructed with Pd metal nanoparticle on carbon and ZnCl<sub>2</sub> that can selectively cleave C–O bonds in a variety of lignin model and lignin under relatively mild conditions (150 °C and 30-300 psi of H<sub>2</sub>).<sup>55</sup> Both Pd/C and Zn<sup>+2</sup> are present the benzyl alcohol and aldehyde groups can be selectively deoxygenated in good yields without hydrogenation of the phenyl ring. Most importantly, monomeric lignin surrogates can be deoxygenated depending on the synergy between the Pd/C and Zn<sup>+2</sup>. β–O–4 linkage of the lignin macromolecule is the most abundant repeating subunit and its selective cleaving such ether linkage undergoing HDO by using Pd/C–Zn<sup>+2</sup> system provided a mean of unfolding the complex polymeric structure of lignin into small molecules of fuel value (Figure 3, eqn. 1). In this model compound guaiacylglycerol–β–guaiacyl ether was hydrogenated and deoxygenated at 150 °C under 20 bar of hydrogen using Zn/Pd/C in MeOH yielding primarily two products guaiacol and 2-methoxy-4-propylphenol (Figure 5, eqn. 1). Catalyst performance was tested for the β–O4 synthetic lignin polymer (*M<sub>n</sub>* 3390, *DP<sub>n</sub>* 12.1) which undergone cleavage and deoxygenation (Figure 3, eqn. 2). EXAFS and XANES studies confirmed that the 30% of the metallic nanoparticles are oxidized and EXAFS studies also confirmed that there is no existence of Pd–Zn bimetallic alloy however at higher temperature (250 °C) XANES and Pd K-edge suggest a small amount of Pd–Zn alloy formation. The investigation of chemical aspects of deoxygenation revealed that Zn adsorption on carbon,

most likely onto –OH sites, and not forming a Pd–Zn alloy or direct Pd–Zn interaction was very different as revealed from XAS studies. Hypothesis given by authors based on the evidences, suggests, Zn<sup>+2</sup> participates in one of two ways, either activate substrate via binding to OH groups inducing reactivity with Pd–H on the surface via hydrogen spillover or alternatively Zn<sup>+2</sup> ions desorbed into solution at the reaction temperature (150 °C). Zinc binds the substrate and activates its cleavage upon encountering Pd–H sites on the catalyst surface. Once the reaction mixture is cooled, the Zn<sup>+2</sup> ions are readsorbed onto the C surface. However, Zn/Pd/C was found to be more effective for the cleavage of β–O–4 linkage of lignin molecules and subsequent HDO of aromatic fragments without any chemical change in aromatic functional groups. The system is capable of removing alcohol oxygen atoms on the alkyl chains and maintain valuable aromaticity and thus useful for cleaving recalcitrant ether bonds of model lignin dimer and polymers.

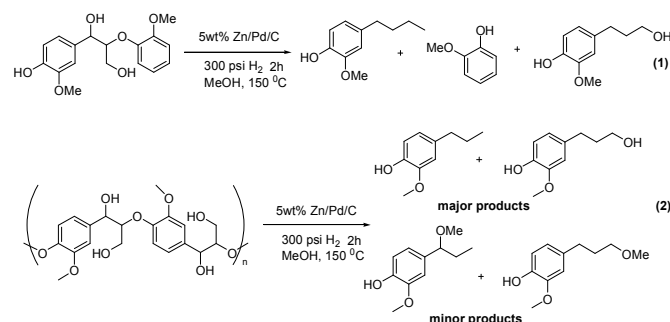


**Figure 5.** β–O–4 dimeric and polymeric lignin cleavage and HDO to remove ether oxygen using Zn/Pd/C system in methanol.

With the initial development of lignin depolymerization chemistry, deoxygenation via the selective hydrogenolysis of C–O bonds has been realized as a key strategy. Dispersed and immobilized nanoscale metal catalysts with dual functionalities plays a significant role in hydrogenolysis of C–O bonds.<sup>56</sup> In this regard, understanding the nature of active sites in such bifunctional catalyst and reaction pathways of C–O bond scission are essential to be addressed. How superior a bimetallic catalysts can act on hydrogenolysis of lignin C–O bond was witnessed in a β–O–4 type C–O bond hydrogenolysis of a lignin model compound 2-phenoxy-1-phenethanol with an optimized 85% Ni and 15% Ru composition.<sup>57</sup> This bimetallic system contains near-surface Ru in the Ni<sub>85</sub>Ru<sub>15</sub> however X-ray absorption and photoelectron spectroscopic results suggest that electron-enriched Ni atom preferentially occupies at the surface studies. Hydrogenolysis results at various temperature and H<sub>2</sub> pressure led authors to conclude that enhanced activation of H<sub>2</sub> and substrate due to electron-rich Ni at the surface was major responsible factor for higher activity than the single component metal catalysts. Using the Ni<sub>85</sub>Ru<sub>15</sub> system, organosolv lignin from *Betula platyphylla* suk, shows that monomeric products can be achieved under the typical reaction conditions as noted in Table 3 in which case the entire process can be investigated by measuring the intensity of C–O bond vibration in the guaiacyl unit and nonconjugated C=O vibration using FTIR spectroscopy. This method of NiRu bimetallic system at optimized ratio of two metals suggests the importance of such species in other processes which it is required to prevent hydrogenation of aromatic ring, in which one of the metal component is more active when used as single metal component.

**Table 3.** Organosolv lignin depolymerisation over Ni, Ru, Ni85Ru15 catalyst in aqueous medium (reaction conditions: 50 mg of organosolv lignin, 3 mL aqueous solution containing 0.22 mmol metal and 0.44 mmol PVP, 10 bar H<sub>2</sub>).<sup>41</sup>

Catalyst	Time (h)	Yield (wt%)			Residual lignin (wt%)
		1	2	3	
Ni	1	0	0	0	46
Ru	1	0.1	0.03	0.03	50
Ni <sub>85</sub> Ru <sub>15</sub>	1	0.1	0.6	0.1	58
Ni <sub>85</sub> Ru <sub>15</sub>	12	1.4	5.0	0.4	56
Ru	12	0.2	0.06	0.6	38

Further interesting feature was reported in the case of NiAu catalyst for the hydrogenolysis of lignin into phenolic chemicals with high selectivity for the  $\beta$ -O-4 type C-O bond hydrogenolysis where with an optimum Ni: Au 7:3 offers 99% conversion of lignin model 2-phenoxy-1-phenylethanol with maximum 87% monomer yield when dimers were reaction intermediates.<sup>58</sup> The comparative TOFs of initial hydrogenolysis results confirms the more active Ni<sub>7</sub>Au<sub>3</sub> catalysts with more active surface sites and increased dispersion. From the EXAFS, XPS, ICP-MS, UV-Vis experiments, authors proposed that the structure of the NiAu catalyst would a Ni enriched Ni-Au shell encapsulates Au core (Figure 6(a)). The exceptional performance of the NiAu catalyst at a Ni: Au = 7:3 may be related to the unique electronic state of Ni where an electronic modification of bimetallic species Ni<sub>7</sub>Au<sub>3</sub> can be revealed from XANES spectra (Figure 6(b) where white light intensity of Au increased with increasing Ni loading, pointing a decreased electron density of Au atoms while interacting with Ni which results a concurrent shift of Ni absorption edge towards a lower energy as Au content increases. In this case Au act as electron donor in NiAu catalyst, enabling neighboring Ni atoms to be more electron enriched which is useful for lignin hydrogenolysis. Upon applying for hydrogenolysis of organosolv lignin, average molecular weight dramatically decreases due to the hydrogenolysis exhibiting complete depolymerization. This case of manipulation of electronic properties of one component of a bimetallic system (Ni) in enhancing overall activity revealed by spectroscopic studies has larger implication on future system design for lignin valorization.

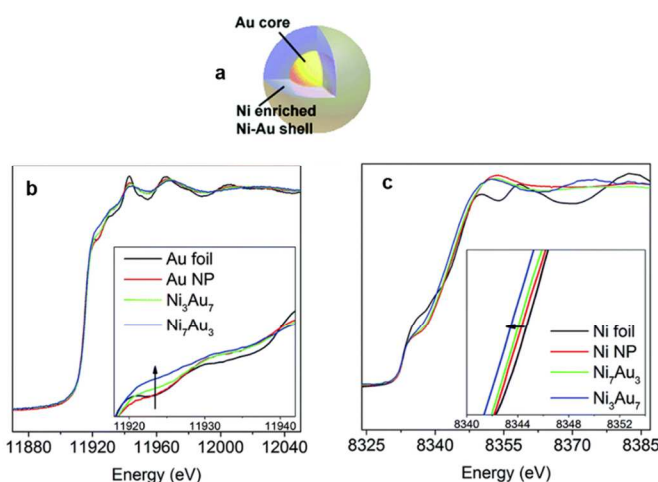


**Figure 6.** (a) Proposed structural representation of NiAu catalyst. (b) Normalized XAS spectra at Au LIII edge of Au, Ni<sub>3</sub>Au<sub>7</sub> and Ni<sub>7</sub>Au<sub>3</sub> catalysts. A spectrum of Au foil was included as a reference; (c) normalized XAS spectra at Ni K edge of Ni, Ni<sub>3</sub>Au<sub>7</sub> and Ni<sub>7</sub>Au<sub>3</sub> catalysts. A spectrum of Ni foil was included as a reference. (Figure 6a, 6b, 6c are reproduced with permission, Copyright Royal Society of Chemistry, 2014).

In addition to develop and explore new combinations of catalyst capable of controlled HDO, studies on oligomeric lignin in order to identify new combinations of catalyst matrixes with multi-catalytic functionalities suitable for efficient depolymerization the lignin polymeric framework into monomeric intermediate and subsequent removal of oxygen via HDO process requires analysis of inter-unit linkages. For example, a recent study revealed, for technical grade lignin to produce C7 to C9 monomeric lignin intermediate under HDO conditions with 5% noble-metal (Ru, Rh, Pt)/Al<sub>2</sub>O<sub>3</sub> (or C)-zeolyst (e.g. NH<sub>4</sub><sup>+</sup> Z-Y 57277-14-1) catalyst matrix.<sup>59</sup> This multi-functional catalyst matrixes showed promising selectivity in conversion of lignin to aromatic hydrocarbons (alkyl benzene derivatives) from a wide variety of lignins under HDO conditions in aqueous media. Results show that the Al<sub>2</sub>O<sub>3</sub> supported noble metal catalysts are effective in reducing functional groups (e.g. methoxyl groups) in lignin aromatic molecules, but are rather inactive for the hydrogenation of the aromatic ring. Thus under HDO conditions, Al<sub>2</sub>O<sub>3</sub> supports are preferable over the carbon supports under different HDO conditions with noble metals (Ru, Pt, Rh) and acidic zeolites (CBV 28014 CY 1.6 and NH<sub>4</sub><sup>+</sup> Z-Y 57277-14-1) in the presence of hydrogen to further improve the yields and selectivity for the production of aromatic hydrocarbons (alkyl benzene derivatives) for incorporation into commercial jet fuels to increase the bulk density and lower cloud point of the fuels. Replacing the acidic zeolite CBV 8014 CY 1.6 with NH<sub>4</sub><sup>+</sup> Z-Y 57277-14-1 was shown to enhance aromatic hydrocarbons and the product selectivities with the noble metals Rh and Pt on Al<sub>2</sub>O<sub>3</sub> supports under HDO conditions. The high reactivity of technical grade lignin based on their sub-structures (Figure 7) accounted for their high reactivity as substrates for HDO reactions. Lignin structure predominantly comprising of 8-O-4' inter unit linkages (C-O-C bonds) would undergo both hydrogenolysis and deoxygenation via cleavage and simultaneous removal of oxygen in the presence of noble metal integrated zeolite catalyst matrix.

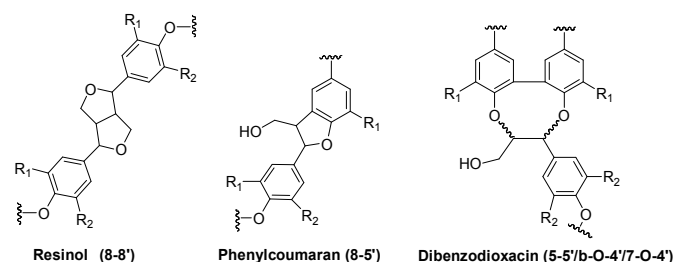


**Figure 7.** Inter-unit linkages based sub-structures of technical grade lignin.

Various analysis of lignin model compounds and distribution of products obtained during the lignin aqueous phase reforming revealed that lignin depolymerization through the disruption of the abundant  $\beta$ -O-4 linkages and less extent, the 5-5' carbon-carbon linkages to form monomeric aromatic compounds is well known,<sup>60</sup> however less efforts has been invested for developing selective HDO techniques to access hydrocarbons from lignin or lignin model compounds. In this context, a combined depolymerization and (hydro)-de-oxygenation of lignin in a single step to access phenolic product over a Pt catalyst with formic acid (H<sub>2</sub> source) can significantly reduce molecular weight and oxygen content.<sup>61</sup> However, this single-step disassembly of lignin offers monomeric cyclohexyl derivatives and aromatic products.<sup>62,63</sup>

A combined depolymerization and HDO of lignin in a two steps using Pt/Al<sub>2</sub>O<sub>3</sub> (ethanol/water) and CoMo/Al<sub>2</sub>O<sub>3</sub> under high

pressure of H<sub>2</sub> was reported for the organosolv and kraft lignin which involves liquid-phase reforming, extraction of lignin-oil and further subject to a HDO step to access deoxygenated products i.e. mono-oxygenated phenolics (Figure 8).<sup>64</sup> It happens that, without a pretreatment step, HDO process with Mo<sub>2</sub>C/CNF (carbon nano fiber) on organosolv lignin offers only small percentage of monomeric phenolics (Figure 9). In spite of positive temperature effect on reducing oxygen content of HDO-derived products, required level of success for hardwood lignin is yet to be achieved which must include a convenient pre-treatment step.

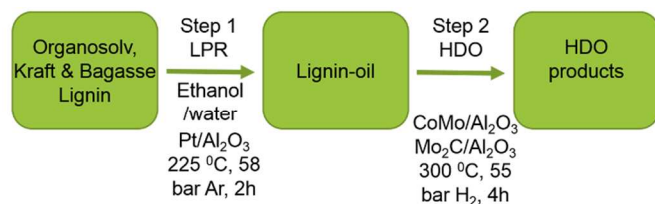


**Figure 8.** Two-step approach to valorization of lignin involving HDO.

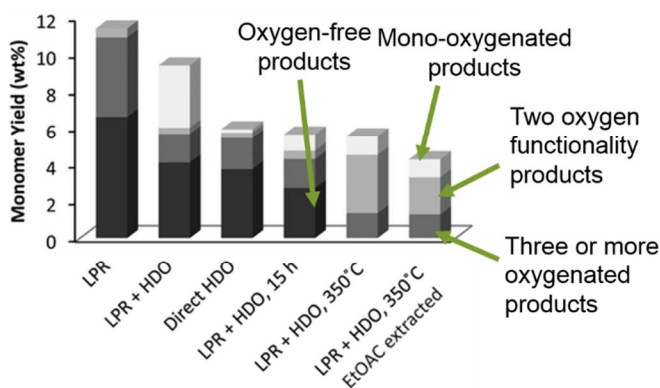


**Figure 9.** Yield of monomeric aromatic products after HDO of organosolv lignin-oil over Mo<sub>2</sub>C/CNF catalyst under different conditions including

### 2.3 Enzymatic Oxidation

Generally, chemical methods to depolymerize lignin generate low yields of complex mixtures of products and also results in the formation of insoluble high molecular weight products. Initially, microbial degradation of lignin has been investigated primarily in white-rot and brown-rot fungi depending on the ability of these fungi to produce extracellular lignin peroxidase and Mn peroxidase enzymes for oxidizing lignin. It was revealed that fungi use iron and redox mediators to carry out Fenton oxidation to depolymerize lignin.<sup>65</sup> Although fungal lignin deconstruction has been studied since long however there is no commercial biocatalytic process involving this technique to date.<sup>66</sup> Several bacterial strains are also able to break down lignin, including actinobacteria such as *Streptomyces viridosporus* which produces an extracellular peroxidase, certain pseudomonads, and the anaerobic bacterium *Enterobacter lignolyticus* SCFI. In *Rhodococcus jostii* RHA1, whose genome sequence has been determined, we have reported the identification and characterization of peroxidase DypB, which can oxidize lignin models, Kraft lignin, lignocellulose, and Mn<sup>2+</sup>.<sup>67</sup> Two further bacterial peroxidase enzymes have been reported from *Amycolatopsis* sp. 75iv2: a heme-containing enzyme capable of oxidizing lignin model compounds<sup>68</sup> and a Dyp2 peroxidase enzyme with higher catalytic activity for Mn<sup>2+</sup> oxidation.<sup>69</sup> Synthetic biology is

finding importance in designing new biosynthetic routes to alkanol, biodiesel, and biofuels as non-fermentative pathway.<sup>70</sup> It was previously observed that *R. Jostii* RHA1 DypB (lignin oxidizing enzymes) is able to cleave a  $\beta$ -aryl ether lignin model compound to produce vanillin and a two-carbon fragment glycoaldehyde. The other aromatic metabolite, 5-carboxyvanillic acid (2), is a potential intermediate in the biphenyl catabolic pathway and can decarboxylated to form vanillic acid for growth.<sup>71</sup> Thus vanillic acid catabolic pathway might be important for lignin breakdown.

For vanillic catabolic pathway, desired would be production of vanillin from lignin component of lignocellulose using gene deletion and the process can be engineered for the production of aromatic compounds. This concept has an advantage of generating small number of metabolites in predictive way which requires a robust organism for which mutant strain growing to high cell density which also prevents formation of toxic aldehyde metabolites. A gene deletion strain of *R. Jostii* RHA1 in which vanillin dehydrogenase gene had been deleted, when grown on minimal medium containing 2.5% wheat straw lignocellulose and 0.05% glucose, offers vanillin as product.<sup>72</sup> A hypothetical catabolic pathways in *R. jostii* RHA1 for breakdown of  $\beta$ -aryl ether and biphenyl components of lignin, based upon the structure of observed metabolites is depicted in Figure 10.

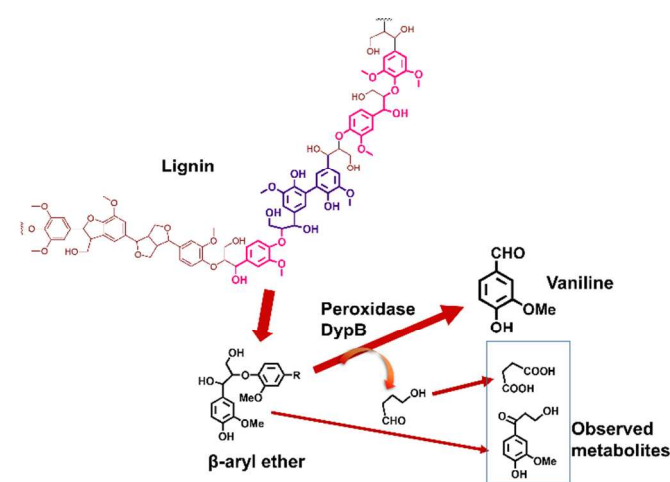


**Figure 10.** Hypothetical catabolic pathways in *R. jostii* RHA1 for breakdown of  $\beta$ -aryl ether and biphenyl components of lignin, based upon the structures of observed metabolites.

Synthetic biology has been used in *Escherichia coli* to engineer new biosynthetic routes to alkanol and biodiesel, but thus far there are limited applications toward biomass deconstruction and little use of other bacterial hosts for synthetic biology. Gene deletion mutant based biocatalytic route to access aromatic chemical like vanillin from wheat straw lignocellulose is a step significantly further towards a metabolic engineering based approach.<sup>73</sup>

### 2.4 Carbonization

Bulk synthesis of materials for energy storage from renewable sources using scalable technologies is desired currently. Even though lignin is a major by-product of chemical pulping and increasingly available for biofuel production, in spite of chemical heterogeneity and structural variations, lignin's high



carbon content and phenolic structure make it an excellent alternative source of carbon materials (Figure 11). Additionally, high mass retention characteristic of lignin in thermal processing has been witnessed in its conversion to carbon fibers (CFs),<sup>74,75</sup> porous activated carbon particles (PAC),<sup>76-78</sup> and graphitic form of CFs. Lignin based CFs contains comparable mechanical properties to commercial polyacrylonitrile-based CFs for reinforcing composites.

Novel microstructured carbon materials find applications as adsorbents and anode materials for battery or supercapacitor.<sup>79</sup> Thus it is highly interesting to devise synthesis technique to access microstructured carbon materials from lignin involving fiber processing and chemical modifications.

#### 2.4.1 Carbon Fibers

The first report on the use of lignin as precursor for carbon fibers deals with conversion of lignin into functional polymers to obtain a spinnable material and fibers after thermal stabilization followed by carbonization.<sup>80</sup> In contrast to the approach based on the use of binder polymer, straightforward method of obtaining carbon micro and nanofibers by the co-electrospinning Alcell lignin solutions at room temperature followed by thermal stabilization and carbonization to produce carbon fibers was reported.<sup>81</sup> Alcell lignin electrospun nanofibers (ALFs) were stabilized by thermal treatment in air at room temperature to 200 °C for 24 h which offers fibers of similar size and then this was carbonized to obtain carbon nanofibers at 900 °C. The carbon crystallites with a preferred orientation along the fiber axis results smooth fiber surface. The fiber remain in the glassy state ( $T_g > T$ ) and the structural organization in the carbon nanofiber was revealed with Raman Spectroscopic study which tells that a lower contribution of structural disorder in the higher-temperature and graphitic carbon formation ( $E_{2g}$ , 1575  $\text{cm}^{-1}$ ) confirmed an onset structural organization. The fiber was found to be oxidation resistant and highly microporous and large micropore volume makes this nanofibers suitable for  $\text{CO}_2$  adsorption-desorption process.

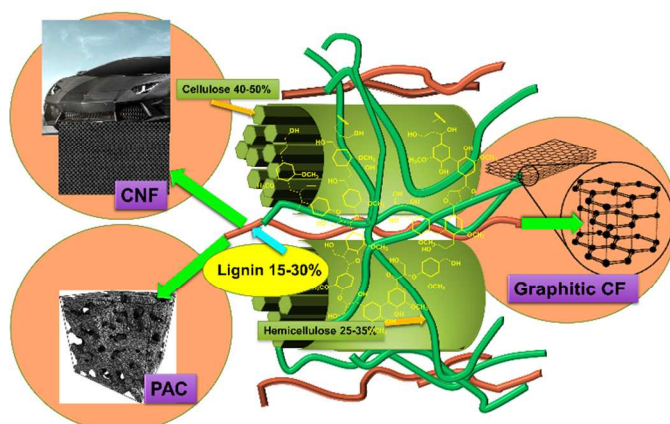


**Figure 11.** Pictorial depiction of lignin as potential source for the various nanostructured carbon materials suitable for advanced technological applications.

A rapid freezing process of aqueous lignin solution, followed by sublimation of the resultant ice forms a uniform network comprised of individual interconnected lignin nanofibers and carbonization of that offers similarly structured carbon nanofiber network.<sup>82</sup> The rapid freezing process resulted in the elimination of larger spaces and macropores observed

due to the formation of smaller ice crystals. Smaller and uniform fiber diameters were generated due to the more rapid heat removal and uniform cooling rates resulting lignin and subsequently individual carbon fibers with diameter less than 100 nm (Figure 12). Fibers tend to have preferential alignment in the direction of freezing front which depends on the concentration.

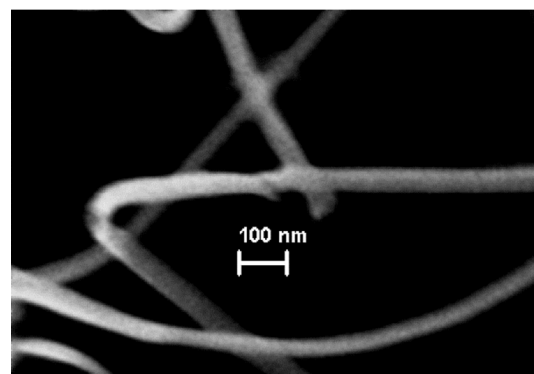


**Figure 12.** Scanning electron micrograph of carbon nanofibers. Individual CNFs derived from lignin with diameters of less than 100 nm. (Reproduced with permission from reference 82, copyright American Chemical Society, 2012).

It has been demonstrated that the conventional graphitic anode of lithium ion batteries can be replaced with lignin carbon fibers (LCFs) when synthesized and applied as monolithic fused mats which contain specific charge capacities.<sup>83</sup> LCFs carbonized at 1000 °C has specific charge capacities. In this case, irreversible lithium insertion and extraction was witnessed in the more disordered LCFs carbonized at 1000 °C with the smallest nanoscale graphitic domains. The question is why we need graphitic domain in a carbon fiber which can enhance the performance of the battery. This happens due to the reason that carbonized structure is modulated to yield an active material with internal mesostructure consisting of high density, nanoscale crystalline (graphitic) domain surrounded by a continuous, low-density, highly disordered carbon matrix. This amorphous carbon enables facile, isotropic lithium transport throughout the fiber structures, providing access to charge storage sites within the nanoscale graphitic domains.<sup>84</sup> It was found that the matrix graphitization increased with the increase in carbonization temperature, i.e. long-range graphite order with no preferential orientation along the fiber axis as shown in SEM image of typical LCF fused mats after carbonization and varying level of fiber-fiber fusion (Figure 13) in which the mat densities can be controlled. The mats are excellent anode materials exhibiting tunable electrochemical performance suitable for high energy applications. The synthesis method results electrically interconnected 3D architecture from lignin 3D structure and final carbon fiber acts as current collector and Li insertion materials. This carbonized lignin has disordered nano-crystalline microstructure.

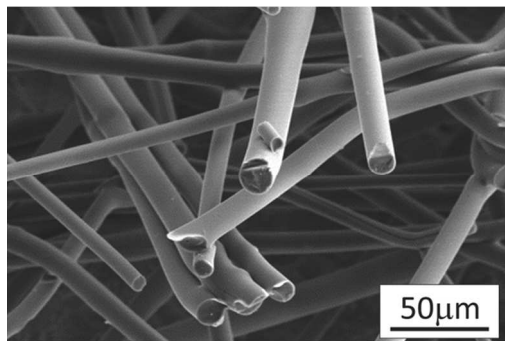


**Figure 13.** SEM image of varying levels of fiber-fiber fusion in LCF mats. (Reproduced with permission from reference 83, copyright Wiley-VCH, 2014)

Structural modification of lignin with different ester groups which results a precursor highly compatible with melt processing technique for fiber extrusion and further conversion into microstructured carbons by oxidative stabilization and subsequent carbonization.<sup>85</sup> The acid anhydride modification of lignin hydroxyl groups (acyl substitution) under neutral condition and under a long reaction time (6h), most of the available (phenolic and aliphatic) hydroxyl groups of lignin would be esterified however that wouldn't change the polymeric structural characteristics of lignin throughout the modification process. Interesting is that the surface areas of resulting carbon materials falls in the range of commercial graphitic carbons. Phthalic anhydride modified lignin contains relatively higher microscale porosity as compared to the unmodified lignin based carbon fiber (Figure 14). This modification influenced on the underlying meso- and microstructure development and pore creation and the carbonization temperature can be adjusted to access carbons with either more graphitic or disordered structures.

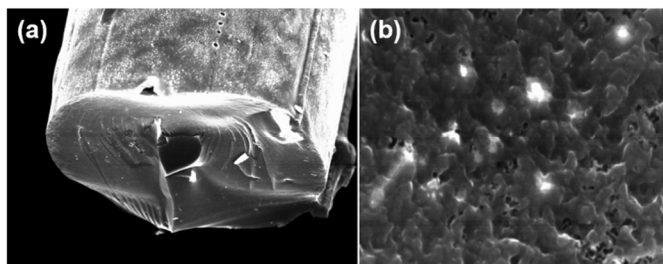


**Figure 14.** Scanning electron micrograph of carbons from (a) phthalic anhydride modified lignin and (b) micro scale porosity of phthalic anhydride modified lignin. (Reproduced with permission from reference 85, copyright RSC, 2013)

Devising methods for ultrafine (100-500 nm) highly porous activated carbon fibers (ACFs) by the electrospinning of aqueous solutions of predominantly alkali lignin (low sulfone content) followed by simultaneous carbonization and activation.<sup>86</sup> The major advantage of this process is the simultaneous carbonization and activation in a single heating step which resulted a range of micropore- to mesopore dominant ACFs with superior specific surface and porosity tuned by varying the contents of alkali hydroxides. Use of the electrospinnable PEO carrier as one ninth of the AL<sub>1s</sub> turned the mixture electrospinnable into fibers. Interestingly, size variation of fibers in 100-300 nm and 300-500 nm range when using NaOH and KOH can also be achieved (Figure 15). The decreased fiber sizes are generally attributed to the increased

charges of the solutions and improved charge dissipation with the added electrolytes in electrospinning.

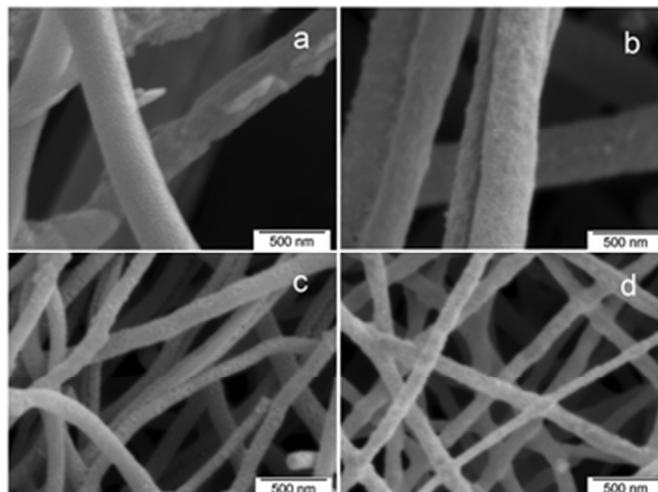


**Figure 15.** SEM images of AL<sub>1s</sub>-PEO hybrid fibers with NaOH (a, b) and KOH (c, d). (Reproduced with permission from reference 86, copyright RSC, 2014)

This approach offers highly porous and high specific surface ACFs with both mesopores and micropore with different size proportions with slit-like micropores at 0.1 impregnation ratio, developed into a network of larger mesopores connected or embedded within the micropores matrix by narrow necks as the ratios increased to 0.3 and 0.5 along with increase of mesopores.

Production of carbon fiber by mixing carbon nanotubes with the carbonaceous precursor to generate carbon nanotube composite fibers and this depends on the chemical modification of the carbonaceous precursors and in this case anhydride compounds plays a special role which turns functionalized lignin suitable for fiber production.<sup>87</sup> This carbon fibers derived from lignin contains controllable turbostatic disorder which is controllable by the choice of functional agent and aspect ratio. In addition, fibers can be derived with desired transport and interfacial properties. These lignin derived fibers found potential applications in Li-ion batteries.

Melt-spinning is already proved as a suitable technique to access carbon fiber and when lignin was modified chemically and blended with poly(lactic) (PLA) before melt-spinning into lignin fibers.<sup>88</sup> This pre-carbonization functionalization involves butyration to form ester functional groups in place of polar hydroxyl (-OH) groups, which enhances the miscibility of lignin with PLA. Microstructure analysis (SEM and TEM) of carbon fibers produced from lignin/PLA blends revealed the composition dependent microporous structure inside the fine fibers (Figure 16). The microvoids in the cross section of all fibers, which is absent in pure lignin derived fibers, produced by PLA after carbonization and size of the microvoids decreased with the increase in lignin content.

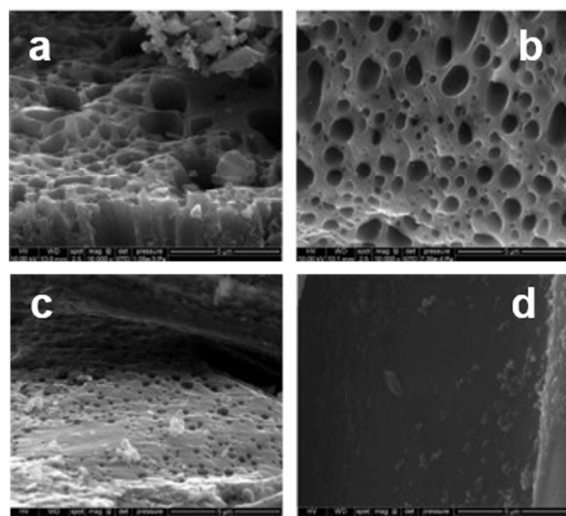


**Figure 16.** SEM images of cross-section of carbon fibers from B-lignin/PLA blends, (a) 50/50; (b) 75/25; (c) 90/10; (d) 100/0. (Reproduced with permission from reference 88, copyright Elsevier, 2014)

A strategy of porous core construction has been witnessed in case of controlled co-electrospinning and carbonization method of lignin and cellulose which produces core-shell carbon fibers with cellulose nanofibrils (CNFs) with porous core. After carbonization a hollow fiber structure was obtained with increased surface and porosity.<sup>89</sup> It is advantageous that increased surface area and porosity extended via co-electrospinning method provides improved platform for various interactions between fibers and their surrounding environments which potentially enhanced the performance of the fibers for advanced applications. Core-shell CNF-lignin/PAN fibers exhibit relatively smooth surfaces where porous core consisted of CNF network and shell consists of lignin and LAN. Difference of lignin based hollow fiber (lignin/PAN) and CNF-lignin based core-shell fiber (CNFs-lignin/PAN) can be easily found while considering cross sectional surface as shown in Figure 17.

In the past and currently, phenolic resin has been broadly applied as source of activated carbon fibers (ACFs), and the lignin with phenyl-propane structure similar to the phenol-formaldehyde resin, is found to be ideal replacement to prepare phenolic resin. Furthermore, application of this resin to fabricate lignin-based carbon materials of controllable surface and pore structure and physical properties are desired.

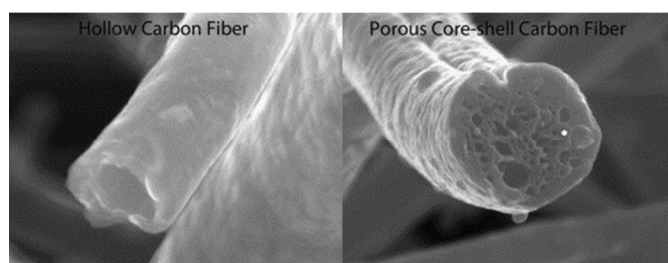


**Figure 17.** SEM images of hollow and porous core-shell carbon fibers derived from lignin/PAN and CNF-lignin/PAN respectively. (Reproduced with permission from reference 89, copyright Elsevier, 2013)

#### 2.4.2 Microporous Carbon

Nanostructured carbons with hierarchical pore arrangement are considered as one of the most appropriate electrode materials for high-performance electrochemical capacitors. The ordered mesopores network of these materials provide shorter diffusion pathways along the carbon particles, which enhances diffusivity of molecules and/or ions to make the inner surface more accessible than the microporous activated carbons. The presence of certain oxygen surface groups on carbon materials can contribute significantly to the performance by improving the wettability of the surface and enhancing pseudocapacitance. Preparation of hierarchically porous carbon from biomass sources is an emerging area of further investigation. The technique to access such novel nanostructured carbons majorly depends on nanocasting technique using hard or soft template. Microporous carbon with a 3D connected and ordered pore structure can be produced by liquid phase impregnation (LPI) with a carbon precursor over a porous zeolite and further template is traditionally removed by HF washing. To prepare ultraporous carbon use of zeolite template and lignin as carbon precursor to obtain zeolite-template carbons (ZTC) containing finger print of zeolite was been achieved recently.<sup>90</sup> This lignin derived ZTCs contains a bimodal pore structure where microporosity results from both removal of zeolite walls and the lignin carbonization, and a mesoporous network is originated as a result of the incomplete pore filling of the hard template. The interesting part is to analyse the origin of mesoporosity for the template carbon materials which replicate both the external and internal morphology of the corresponding zeolite crystals.

### 3. Summary and Outlook

We have reviewed recent work on a number emerging strategies of lignin valorization including, depolymerizations into monomers, further upgradation of monomers, enzymatic oxidation, and carbonization. Among these, depolymerisation via hydrogenolysis of lignin into monomers has been the key strategy however, with the development nanoscale catalyst, selective deoxygenation via the hydrogenolysis of  $\beta$ -O-4 type C-O bond has emerged as a challenging target for further upgradation of monomers obtained via lignin depolymerization. Emerging strategies of enzymatic oxidation of lignin is reviewed with limited case along with covering the potentials of lignin for the production of carbon materials of a wide range of nanostructures.

As a resource of nanomaterials, biopolymers have many advantages and can be extracted industrially on a large scale, for example, lignin from kraft pulping.<sup>91</sup> Some of the current approaches showed that lignin can be versatile source to obtain high quality wide range of nanostructured carbon fibers which are emerging materials for the electrochemical energy storage applications. The article has also analyzed the scope of the deoxygenation techniques for upgradation of lignin-derived aromatic functionalized monomers and its successful recent outcomes for accessing high value deoxygenation products containing the intact aromatic ring. However, lignin depolymerization from intact biomass currently produces a largely heterogeneous slate of molecules, which makes lignin valorization an enormously difficult problem. Such strategies of cleavage of polymeric units consists of aromatic fragments demonstrate the careful selection of reactive molecules or nanoparticles capable of selective cleavage of biomass lignin. This makes a successful route to disrupt the recalcitrance of lignin under controlled conditions to generate value from lignin

and to make carbohydrate fraction more reactive for hydrolysis. Enzymatic strategies involving synthetic biological processes involving appropriate enzymes are currently evolving and has lot to offer. In nature, lignin is slowly degraded by white-rot fungi such as *Phanerochaete chrysosporium*, which provides an extracellular lignin peroxidase enzyme to begin the degradation process. Manganese peroxidase and laccase enzymes that are also capable of lignin breakdown to initial breakdown products such as phenylpropanoid dimers which can be further degraded via aromatic meta-cleavage pathways and this is carried out in nature by soil bacteria. Certain studies that contain huge potential to change the face of lignin valorization are envisaged as follows,

1) Accessing non-pyrolytic lignin bio-oil by developing new depolymerisation strategy is essential since the lignin-bio-oil is extremely amenable to HDO for further upgradation, and therefore a catalytic biorefining method can be established. Transfer hydrogenation in alcohol media has found as a potential strategy as discussed earlier in this article. New hydrogen transfer strategy under mild condition will be sorted for the future development of depolymerisation process to access lignin-oil-fraction. Efficient strategies would enable to proceed by avoiding the use of recalcitrant solid polymer obtained from organosolv process.

2) Establishing the role of bimetallic alloy system for selective C–O bond hydrogenolysis is one of fundamental interests related to lignin valorization and its chemical aspects. Development of strong and effective homogeneous catalyst for HDO is something are not often witnessed recently. This topic has significant scope for developing new lignin chemistry. Moreover, in HDO of naturally occurring lignin species, what features of lignin surface and its role will be important, that is yet to be revealed. In plenty of ways, HDO process are to be studied extensively in future in addition to design and improve conventional methods of lignin depolymerization.

3) Identify new bacterial lignin degraders and test enzymes like manganese peroxidase and laccase in solution phase and immobilized phase. Mechanism of lignin cleavage by enzymes is an interesting area to explore. Polysaccharide monooxygenase enzyme AA9 (GH61) is also another candidate for the lignin valorization.<sup>92</sup> In this respect, bacterial peroxidase enzymes are potential bet which are capable of oxidizing lignin.<sup>93</sup> The article highlight this part is because to convey the message that experts of biology has a major role to play in near future for the gene specific or gene altered enzyme specific disruption of biopolymer chain of lignin. Apart from exploring new oxygenase enzymes, novel nanomaterials-enzyme composites and enzyme encapsulated nanoscale materials as biocatalysts should be explored and this offers a potential area develop lignin chemistry.

4) The strategy of exemplifying the potential of different rigid templates such as hierarchical zeolites and large pore metal-organic frameworks can be extensively tested for the access of hierarchical porous carbon (HPC) by infiltration of lignin as carbon source. Novel strategies to obtain carbon by using lignin as carbon precursor has plenty to offer for design and develop energy storage devices. In order to develop strategies of chemical modification or chemical conversion of lignin, it is high important to considered the bonds which are to be cleaved.

### Acknowledgements

SD and KWC Wu thank the Ministry of Science and Technology (MOST), Taiwan (101-2628-E-002-015-MY3,

101-2623-E-002-005-ET, 101-2923-E-002-012-MY3, 103-2811-E-002-018 and 103-2218-E-002-101), National Taiwan University (101R7842 and 102R7740), and the Center of Strategic Materials Alliance for Research and Technology (SMART Center) of National Taiwan University (102R104100) for funding supports. BS acknowledges the Center for Direct Catalytic Conversion of Biomass to Biofuels (C3Bio), an Energy Frontier Research Center funded by the U. S. Department of Energy, Office of Science, and Office of Basic Energy Sciences under Award Number DE-SC0000997 for the financial support.

### Notes and references

<sup>a</sup> Department of Chemical Engineering, National Taiwan University, Taipei, Taiwan 10617. E-mail: saikatdutta2008@gmail.com

<sup>b</sup> Center for Direct Catalytic Conversion of Biomass to Biofuels (C3Bio), Department of Chemistry and Energy Center, Purdue University, West Lafayette, IN 47907 USA.

<sup>c</sup> Brown Laboratory, Department of Chemistry and School of Chemical Engineering, Purdue University, 560 Oval Drive, West Lafayette, USA.

† Footnotes should appear here. These might include comments relevant to but not central to the matter under discussion, limited experimental and spectral data, and crystallographic data.

Electronic Supplementary Information (ESI) available: [details of any supplementary information available should be included here]. See DOI: 10.1039/b000000x/

- 1 A. S. Mamman, A. S.; J.-M. Lee, Y.-C. Kim, I. T. Hwang, N.-J. Park, Y. K. Hwang, J.-S. Chang and J.-S. Hwang, *Biofuels, Bioprod. Biorefin.*, 2008, **2**, 438–454.
- 2 R. E. Hage, N. Brosse, L. Chrusciel, C. Sanchez, P. Sannigrahi and A. Ragauskas, *Polym. Degrad. Stab.*, 2009, **94**, 1632–1638.
- 3 H. H. Nimz, *Angew. Chem., Int. Ed.*, 1974, **13**, 313–321.
- 4 E. Adler, *Wood Sci. Technol.*, 1977, **11**, 169–218.
- 5 G. Chatel and R. D. Rogers, *ACS Sustainable Chem. Eng.*, 2014, **2**, 322–339.
- 6 J. Zakzeski, P. C. A. Bruijninx, A. L. Jongerius and B. M. Weckhuysen, *Chem. Rev.*, 2010, **110**, 3552.
- 7 J. Holladay, J. F. White, J. J. Bozell, D. Johnson, DOE Report “Top Value-Added Chemicals from Biomass, Volume II” 2007.
- 8 D. D. Laskar, B. Yang, H. Wang and J. Lee, *Biofuels Bioprod. Bior.*, 2013, **7**, 602–626.
- 9 H. Yang, R. Yan, H. Chen, D. H. Lee and C. Zheng, *Fuel*, 2007, **86**, 1781–1788.
- 10 J. R. Regalbuto, *Science*, 2009, **325**, 822–824.
- 11 V. M. Roberts, V. Stein, T. Reiner, A. Lemonidou, X. Li and J. A. Lercher, *Chem Eur. J.*, 2011, **17**, 5939–5948.
- 12 B. G. Janesko, *Phy. Chem. Chem. Phys.*, 2014, **16**, 5423–5433.
- 13 N. Sathitsuksanoh, K. M. Holtman, D. J. Yelle, T. Morgan, V. Stavila, J. Pelton, H. Blanch, B. A. Simmons, A. George, *Green. Chem.*, 2014, **16**, 1236–1247.
- 14 Z. Ma, E. Troussard and J. A. Van Bokhoven, *Appl. Catal. A. Gen.*, 2012, **423–424**, 130–136.
- 15 P. F. Britt, A. C. Buchanan, M. J. Cooney and D. R. Martineau, *J. Org. Chem.*, 2000, **65**, 1376–1389.

- 16 G. S. Macala, T. D. Matson, C. L. Johnson, R. S. Lewis, A. V. Iretskii and P. C. Ford *ChemSusChem* **2009**, *2*, 215–217.
- 17 Z. Li, M. Garedeew, C.-H. Lam, J. E. James, D. J. Miller and C. M. Saffron, *Green Chem.*, **2012**, *14*, 2540–2549.
- 18 R. W. Thring and J. Breau, *Fuel*, 1996, **75**, 795–800.
- 19 W. L. Schinski, A. E. Kuperman, J. Han and D. G. Nae, US 2009/0218061A0218061, 2009.
- 20 M. Saisu, T. Sato, M. Watanabe, T. Adschiri and K. Arai, *Energy Fuels*, 2003, **17**, 922–928.
- 21 M. Osada, T. Sato, M. Watanabe, T. Adschiri and K. Arai, *Energy Fuels*, 2004, **18**, 327–333.
- 22 M. Osada, N. Hiyoshi, O. Sato, K. Arai and M. Shirai, *Energy Fuels*, 2007, **21**, 1854–1858.
- 23 J. Huang, X. Wang, Z. L. Wang, *Nano Lett.*, 2006, **6**, 2325–2331.
- 24 H. Lange, S. Decina and C. Crestini, *Eur. Polym. J.*, 2013, **49**, 1151–1173.
- 25 Y. Gao, J. Zhang, X. Chen, D. Ma and N. Yan, *ChemPlusChem*, 2014, DOI: 10.1002/cplu.201300439.
- 26 T. Radoykova, S. Nenkova and K. Stanulov, *Chem. Nat. Compd.*, 2010, **46**, 807–808.
- 27 Wahyudiono, M. Sasaki and M. Goto, *Fuel*, 2009, **88**, 1656–1664.
- 28 S. Karagöz, T. Bhaskar, A. Muto and Y. Sakata, *Fuel*, 2004, **83**, 2293–2299.
- 29 T. Voitl and P. Rudolf von Rohr, *ChemSusChem*, 2008, **1**, 763–769.
- 30 K. Stärk, N. Taccardi, A. B'osmann and P. Wasserscheid, *ChemSusChem*, 2010, **3**, 719–723.
- 31 J. Zakzeski, A. L. Jongerius, P. C. A. Bruijninx and B. M. Weckhuysen, *ChemSusChem*, 2012, **5**, 1602–1609.
- 32 R. W. Coughlin and F. Davoudzadeh, *Nature*, 1983, **303**, 789–791.
- 33 N. Yan, C. Zhao, P. J. Dyson, C. Wang, L. T. Liu and Y. Kou, *ChemSusChem*, 2008, **1**, 626–629.
- 34 C. Z. Li, M. Y. Zheng, A. Q. Wang and T. Zhang, *Energy Environ. Sci.*, 2012, **5**, 6383–6390.
- 35 E. E. Harris, J. D'Ianni and H. Adkins, *J. Am. Chem. Soc.*, 1938, **60**, 1467–1470.
- 36 A. L. Jongerius, R. Jastrzebski, P. C. A. Bruijninx and B. M. Weckhuysen, *J. Catal.*, 2012, **285**, 315–323.
- 37 J. M. Nichols, L. M. Bishop, R. G. Bergman and J. A. Ellman, *J. Am. Chem. Soc.*, 2010, **132**, 12554–12555.
- 38 R. C. Runnebaum, T. Nimmanwudipong, D. E. Block and B. C. Gates, *Catal. Sci. Technol.*, 2012, **2**, 113–118.
- 39 Q. Song, F. Wang and J. Xu, *Chem. Commun.*, 2012, **48**, 7019–7021.
- 40 Q. Song, F. Wang, J. Cai, Y. Wang, J. Zhang, W. Yu and J. Xu, *Energy Environ. Sci.*, 2013, **6**, 994–1007.
- 41 J. M. W. Chan, S. Bauer, H. Sorek, S. Sreekumar, K. Wang and F. D. Toste, *ACS Catal.*, 2013, **3**, 1369–1377.
- 42 X. Ma, Y. Tian, W. Hao, R. Ma and Y. Li, *Appl. Catal. A. Gen.*, 2014, **481**, 64–70.
- 43 T. Yoshikawa, T. Yagi, S. Shinohara, T. Fukunaga, Y. Nakasaka, T. Tago, T. Masuda, *Fuel Processing Technol.*, 2013, **108**, 69–75.
- 44 T. Yoshikawa, S. Shinohara, T. Yagi, N. Ryumon, Y. Nakasaka, T. Tago and T. Masuda, *Appl. Catal. B. Env.*, 2014, **146**, 289–297.
- 45 R. Ma, W. Hao, X. Ma, Y. Tian and Y. Li, *Angew. Chem. Int. Ed.*, 2014, DOI: 10.1002/anie.201402752.
- 46 S. Dutta, *ChemSusChem*, 2012, **5**, 2125–2127.
- 47 J. Yi, S. Liu and M. M. Abu-Omar, *ChemSusChem*, 2012, **5**, 1401–1404.
- 48 M. Shiramizu and F. D. Toste, *Angew. Chem.*, 2012, **124**, 8206–8210; *Angew. Chem. Int. Ed.*, 2012, **51**, 8082–8086.
- 49 M. Saidi, F. Samimi, D. Karimipourfard, T. Niannwudipong, B. C. Gates and M. R. Rahimpour, *Energy Environ. Sci.*, 2014, **7**, 103–129.
- 50 S. Crossley, J. Faria, M. Shen and D. E. Resasco, *Science*, 2009, **327**, 68–72.
- 51 J. Wildschut, M. Iqbal, F. H. Mahfud, I. Melian-Cabrera, R. H. Venderbosch and H. J. Heeres, *Energy Environ. Sci.*, 2010, **3**, 962–70.
- 52 J. Wildschut, I. Melian-Cabrera and H. J. Heeres, *Appl. Catal., B*, 2010, **99**, 298–306.
- 53 F. D. Mercader, M. J. Groeneveld, S. R. A. Kersten, C. Geantet, G. Toussaint, N. W. J. Way, C. J. Schaverien and K. J. A. Hogendoorn, *Energy Environ. Sci.*, 2011, **4**, 985–997.
- 54 A. G. Sergeev and J. F. Hartwig, *Science*, 2011, **332**, 439–443.
- 55 T. H. Parsell, B. C. Owen, I. Klein, T. M. Jarrell, C. L. Marcum, L. J. Hauptert, L. M. Amundson, H. I. Kentamaa, F. Ribeiro, J. T. Miller and M. M. Abu-Omar, *Chem. Sci.*, 2013, **4**, 806–813.
- 56 N. Yan and P. J. Dyson, *Curr. Opin. Chem. Eng.*, 2013, **2**, 178–183.
- 57 J. Zhang, J. Teo, X. Chen, H. Asakura, T. Tanaka, K. Teramura and N. Yan, *ACS Catal.*, 2014, **4**, 1574–1583.
- 58 J. Zhang, H. Asakura, J. van Rijn, J. Yang, P. Duchesne, B. Zhang, X. Chen, P. Zhang, M. Saeys and N. Yan, *Green Chem.*, 2014, **16**, 2432–2437.
- 59 D. D. Laskar, M. P. Tucker, X. Chen, G. L. Helms and B. Yang, *Green Chem.*, 2014, **16**, 897–910.
- 60 J. Zakzeski, B. M. Weckhuysen, *ChemSusChem*, 2011, **4**, 369–378.
- 61 W. Y. Xu, S. J. Miller, P. K. Agrawal and C. W. Jones, *ChemSusChem*, 2012, **5**, 667–675.
- 62 K. Barta, T. D. Matson, M. L. Fettig, S. L. Scott, A. V. Iretskii and P. C. Ford, *Green Chem.* 2010, **12**, 1640–1647.
- 63 T. D. Matson, K. Barta, A. V. Iretskii and P. C. Ford, *J. Am. Chem. Soc.* 2011, **133**, 14090–14097.
- 64 A. L. Jongerius, P. C. A. Bruijninx and B. M. Weckhuysen, *Green Chem.*, **2013**, *15*, 3049–3056.
- 65 D. W. S. Wong, *Appl. Biochem. Biotechnol.*, 2010, **157**, 174–209.
- 66 T. D. H. Bugg, M. Ahmad, E. M. Hardiman, and R. Rahmanpour, *Nat. Prod. Rep.*, 2011, **28**, 1883–1896.
- 67 M. Ahmad, J. N. Roberts, E. M. Hardiman, R. Singh, L. D. Eltis and T. D. H. Bugg, *Biochemistry*, 2011, **50**, 5096–5107.
- 68 M. E. Brown, M. C. Walker, T. G. Nakashige, A. T., Iavarone and M. C. Y. Chang, *J. Am. Chem. Soc.*, 2011, **133**, 18006–18009.
- 69 M. E. Brown, T. Barros and M. C. Y. Chang, *ACS Chem. Biol.* 2012, **7**, 2074–2081.
- 70 S. Atsumi, T. Hanai and J. C. Liao, *Nature*, 2008, **451**, 86–90.
- 71 X. Peng, E. Masai, H. Kitayama, K. Harada, Y. Katayama and M. Fukuda, *Appl. Environ. Microbiol.*, 2002, **68**, 4407–4415.
- 72 P. D. Sainsbury, E. M. Hardiman, M. Ahmad, H. Otani, N. Seghezzi, L. D. Eltis, and T. D. H. Bugg *ACS Chem. Biol.* 2013, **8**, 2151–2156.
- 73 J. W. Lee, D. Na, J. M. Park, J. M. Lee, S. Choi and S. Y. Lee, *Nat. Chem. Biol.*, 2012, **8**, 536–546.
- 74 J. F. Kadla, S. Kubo, R. A. Venditti, R. D. Gilbert, A. L. Compere and W. Griffith, *Carbon*, 2002, **40**, 2913–2920.

- 75 J. L. Braun, K. M. Holtman and J. F. Kadla, *Carbon*, 2005, **43**, 385–394.
- 76 J. Hayashi, A. Kazehaya, K. Muroyama and A. P. Watkinson, *Carbon*, 2000, **38**, 1873–1878.
- 77 V. Fierro, V. Torne-Fernandez and A. Celzard, *Microporous Mesoporous Mater.*, 2007, **101**, 419–431.
- 78 K. Babel and K. Jurewicz, *Carbon*, 2008, **46**, 1948–1956.
- 79 W. E. Tenhaeff, O. Rios, K. More and M. A. McGuire, *Adv. Funct. Mater.*, 2013, **24**, 86–94.
- 80 S. Kubo, Y. Uraki and Y. Sano, *Carbon* **1998**, *36*, 1119–1124.
- 81 M. Lallave, J. Bedia, R. Ruiz-Rosas, J. Rodríguez-Mirasol, T. Cordero, J. C. Otero, M. Marquez, A. Barrero, and I. G. Loscertales, *Adv. Mater.*, 2007, **19**, 4292–4296.
- 82 J. Spender, A. L. Demers, X. Xie, A. E. Cline, M. A. Earle, L. D. Ellis and D. J. Neivandt, *Nano Lett.*, 2012, **12**, 3857–3860.
- 83 W. E. Tenhaeff, O. Rios, K. More, and M. A. McGuire *Adv. Funct. Mater.*, 2014, **24**, 86–94.
- 84 M. Park, X. C. Zhang, M. D. Chung, G. B. Less and A. M. Sastry, *J. Power Sources*, 2010, **195**, 7904–7929.
- 85 S. Chatterjee, A. Clingenpeel, A. McKenna, O. Rios and A. Johns, *RSC Adv.*, 2014, **4**, 4743–4753.
- 86 S. Hu and Y.-L. Hsieh, *J. Mat. Chem. A* 2013, **1**, 11279–11288.
- 87 O. Rios, W. E. Tenhaeff, C. Daniel, N. J. Dudney, A. Johns, G. Alexander and F. S. Baker, *US Pat.* 2014/0038034 A1.
- 88 M. Thunga, K. Chen, D. Gewell and M. R. Kessler, *Carbon*, 2014, **68**, 159–166.
- 89 X. Xu, J. Zhou, L. Jiang, G. Lubineau, Y. Chen, X.-F. Wu and R. Piere, *Materials Lett.*, 2013, **109**, 175–178.
- 90 R. Ruiz-Rosas, M. J. Valero-Romero, D. Salinas-Torres, J. Rodríguez-Mirasol, T. Cordero, E. Morallon and D. Cazorla-Amoros, *ChemSusChem*, 2014, DOI: 10.1002/cssc.201301408.
- 91 Z. Schnepf, *Angew. Chem. Int. Ed.*, 2012, **52**, 1096–1108.
- 92 J. Hu, V. Arantes, A. Pribowo, K. Gourlay and J. N. Saddler, *Energy Environ. Sci.*, 2014, DOI: 10.1039/C4EE00891J.
- 93 M. E. Brown, M. C. Walker, T. G. Nakashige, A. T. Lavarone and M. C. Y. Chang, *J. Am. Chem. Soc.*, 2011, **133**, 18006–18009.